Sci. Council Studies, No. 48, 2017, 1–11 Publication (Upload) date: xx Dec 2017

Annual Temperature Curves in Twelve Regions of the Gulf of Maine 1985–2013

Ernest D. True

Department of Mathematics, Norwich University
Northfield, Vermont 05663, USA

TRUE, E. 2017. Annual Temperature Curves in Twelve Regions of the Gulf of Maine 1985–2013. *Scientific Council Studies*, **48**: 1–11. doi:10.2960/S.v48.m1

Abstract

Annual temperature functions have been constructed from historical ocean station data (OSD), expendable bathythermograph (XBT) and conductivity-temperature-depth (CTD) temperature data collected in the Gulf of Maine during the years 1985–2013. The data, from WOD13, was compiled by the Ocean Climate Laboratory (OCL) of the National Oceanographic Data Center/NOAA (NODC). The Gulf of Maine is divided into 12 regions where annual temperature variability may be compared among coastal regions, banks and basins. For each of the 12 regions, annual temperature functions, which are truncated Fourier series, are constructed for a surface layer of 0–30 m and an intermediate layer of 30–70 m. These annual temperature functions are used as benchmarks over this 28 year period so that annual temperature fluctuations can be compared with the historical data of each region. Tables are presented from which the temperature functions may be reproduced, and include the days of the year at which the temperatures obtained an annual maximum and minimum so that annual warming and cooling cycles can be compared among the regions. This work is a continuation of an earlier article in which the same temperature functions were constructed from the NODC data during the period 1912–1983. In most of the 12 regions, the mean annual temperatures for the period 1985–2013 are slightly higher than those of the period 1912–1983.

Keywords: annual temperature curves, banks, basins, Gulf of Maine, water masses

Introduction

The Gulf of Maine (GOM) is a partially enclosed portion of the continental shelf of the northwest Atlantic Ocean. It's temperature and salinity are partially influenced by exterior sources. The colder, fresher, nutrient poor Scotian Shelf Water (SSW) enters as surface water near Cape Sable, Nova Scotia in Canada, and can also flow across Brown's Bank and enter through the east edge of the Northeast Channel. Warm Slope Water (WSW) from the northwest edge of the Gulf Stream enters the Gulf through the east edge of the Northeast Channel at depth, as does the deeper Labrador Slope Water (LSW). The LSW is cooler and slightly fresher than WSW.

The exterior water sources exhibit major interannual variability in temperature, salinity, nutrients and volumes and play a significant role in the makeup of Gulf of Maine waters (Townsend, 2015). For more details on the effect of these water masses, see Li *et al*. (2014a,b), Smith *et al*. (2001), Colbourne (2004), and their references. Locally, seasonal and interannual variability occurs due to changes in precipitation and evaporation, surface wind forcing, heat flux, and freshwater river runoff.

Throughout the 1900s and early 2000s, a number of articles examined the seasonal and long-term temperature variability in the Gulf of Maine and surrounding waters. One data set of surface temperature readings taken twice daily since 1921 at St. Andrews in the Bay of Fundy, New Brunswick, Canada was used by Lauzier (1965) to show a warming period from the 1940s to the 1950s, followed by a cooling trend from the 1950s to 1965. The same data set was later used by Drinkwater and Gilbert(2004), to show another cooling trend in the late 1980s, followed by a temperature increase through the 1990s. They also used the data set of temperatures taken twice daily at Halifax, Nova Scotia since 1926, where surface temperatures rose during the 1990s. On the Scotian Shelf, they also found that near-surface temperatures in 1999 reached its second highest value in 55 years, while salinity values were at a record low value. By 2000, salinity values had returned to normal.

Ji *et al.* (2008) demonstrate how cold low salinity surface water from the Scotian Shelf into the Gulf of Maine reduces vertical mixing, reducing nutrients from rising to the surface to enhance photosynthesis, causing a reduction in net primary production. In late February 1999, during

a cruise across the central Gulf of Maine, Durbin *et al.* (2003) observed a winter phytoplankton bloom which was not present during a similar cruise in February 2000. A large amount of colder, low-salinity SSW was recorded in February 1999 in the Central Gulf, which helped to stabilize the water column and enhance early phytoplankton growth. This, in turn, supported high zooplankton populations. But during the same period in 2000, with no significant presence of Scotian Shelf waters, phytoplankton and zooplankton populations were typically low.

There has also been considerable discussion regarding the influence of external water types entering the GOM and subsequent changes in primary production for the future. In the Gulf of St. Lawrence, Drinkwater and Gilbert (2004) report that the river discharge from the St. Lawrence, Ottawa and Saquenay rivers during 1980–2000 was at its highest in 90 years. Near-surface temperatures in the southern gulf of St. Lawrence have increased since the 1970s, reaching its highest value in 1999 since the 1950s. But subsurface temperatures were generally colder in the 1990s. These waters make up part of the SSW entering the GOM. Townsend *et al.* (2015) report that in recent years Arctic melting has led to increased fresher, colder, less-nutrient fluxes into the Gulf of Maine through the Scotian Shelf current. A larger volume of this nutrient-poor water prevents the inflow through the northern section of the Northeast Channel of the deeper nutrient-rich water masses from the LSW and WSW. This reduction in nutrient rich injections to the GOM leads to a reduction in biological productivity.

The purpose of this study is to use a large accumulation of historical data to construct annual temperature curves in 12 important regions of the GOM from 1985–2013. These annual temperature curves can then be used as benchmarks to compare fluctuations during shorter time periods and in the near future.

Methods

Description of Data

The data used in this study is the historical ocean station data(OSD), XBT and CTD data available from the World Ocean Database 2013 (Boyer *et al.*, 2013). The data is managed by the Ocean Climate Laboratory(OCL), created by the National Oceanographic Data Center (NODC). The data in WOD13 includes work by numerous oceanographers around the world over the years whose data collecting surveys have been conducted with many different objectives. The OCL has processed this data into the same format for convenient access to the public. The quality control and processing of this data is described in "The World Ocean Database 2013 User's Manual" (Johnson *et al.*, 2013). The data includes optional quality control flags, which were used in this study to include only clean casts. Also, the XBT data was corrected following the Gourestki bias correction for XBT data (Gourestki and Kolterman, 2007). The OSD, XBT and CTD temperature data were extracted from the database for the period 1985–2013.

Description of Regions

The Gulf of Maine is partitioned into 12 regions (Fig. 1), based on the topography, basins and banks of importance in biological studies. The New England coastal areas are covered in regions 1 through 3 and 12. Regions 4 and 5 cover the Bay of Fundy and the coastal waters off Nova Scotia from Yarmouth to Barrington Bay and includes Cape Sable Island and Lurcher Shoals. Region 5 is bordered by the offshore areas on the west by Jordan Basin (region 6) and on the south by the north edge of Browns Bank. The regions 7, 9 and 10 cover Georges, Rodgers and Wilkinson Basins, respectively. Region 8 covers Georges Bank within the 80 meter isobath. The offshore area, region 11, which includes Jeffreys Bank, is made up of small basins, ridges and ledges between Jordan and Wilkinson Basins. This particular partition of the GOM is meant to examine temperature variability separately over basins, banks and strong tidal mixing regions along the coast. The seasonal amplitude in temperature differs considerably over the various regions due in part to topography, tidal mixing, river runoff, and atmospheric forcing. The flux of external water masses also plays an important role in some regions. In particular, Jordan and Georges Basin experience temperature changes as a consequence of intrusions of Scotian Shelf waters and warm slope waters (Townsend *et al.*, 2015).

The total number of OSD, XBT and CTD stations used in this study by month for each of the 12 regions is given in Table 1. The data set contains a total of 26,171 temperature stations compared with the 17,499 stations that were used in the 1912–1983 study (True and Wiitala, 1990).

Annual Temperature Curves

For each of the 12 regions, annual temperature curves for the surface layer (0–30 m) and an intermediate layer (30–70 m) were constructed. The procedure is the same as the curves presented in the earlier 1912–1983 study, so that comparisons can be made. For each station in a given region, the temperatures were integrated over a given depth interval to obtain a weighted mean temperature. Only those stations in the data set with three or more temperature readings in the given depth interval were used.

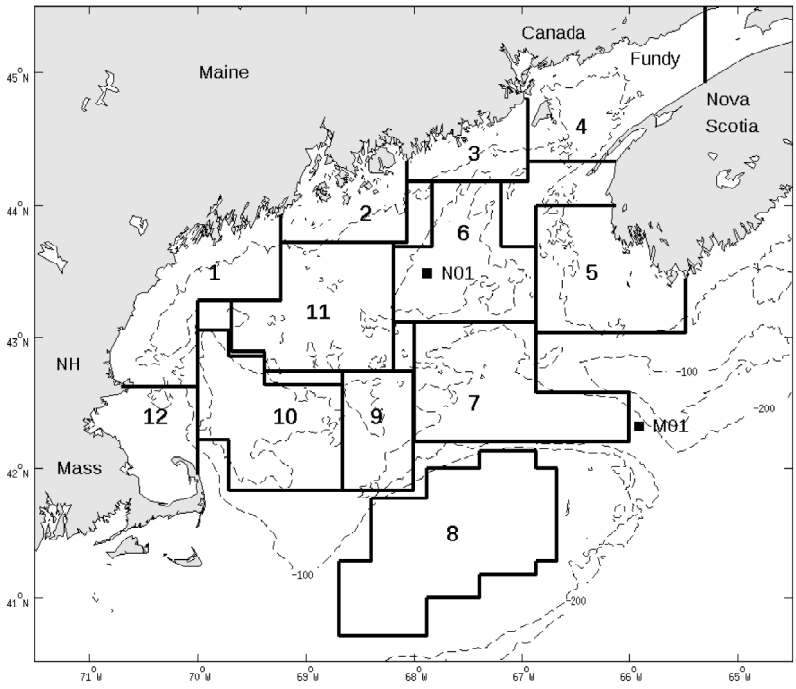

Fig 1. Twelve regions in the Gulf of Maine in which annual temperature curves are presented.

Table 1. The number of ODS, XBT and CTD stations for each month in each Region

Region	Jan	Feb	Mar	Apr	May	Jun	Jul	Aug	Sep	Oct	Nov	Dec	Total
1	30	54	42	291	125	78	220	255	183	298	181	50	1 807
2	9	11	0	131	70	45	68	131	49	76	26	4	620
3	2	11	1	73	9	31	74	106	7	87	118	2	521
4	74	116	100	155	291	252	641	566	254	374	624	267	3 714
5	55	58	61	196	76	137	162	294	101	427	406	43	2 016
6	37	64	16	219	18	141	125	170	49	189	132	9	1 169
7	86	130	90	400	84	263	336	209	280	393	230	55	2 556
8	376	752	522	874	1001	681	390	982	286	832	763	286	7 745
9	36	67	38	136	82	69	35	55	138	151	72	16	895
10	57	103	65	204	82	144	85	136	201	237	149	34	1 497
11	46	97	39	207	67	95	111	204	81	207	141	29	1 324
12	128	169	94	340	79	144	112	240	156	396	293	156	2 307
Total	**936**	**1 632**	**1 068**	**3 226**	**1 984**	**2 080**	**2 359**	**3 348**	**1 785**	**3 667**	**3 135**	**951**	**26 171**

This eliminates stations like those in which only surface temperatures were taken. Next, for each day of the year in which more than one set of station readings occurred, the integrated temperatures were averaged to produce a single mean temperature for that day. This distributes the data more evenly throughout the year and reduces the weighting for the curve fitting scheme which followed. The resulting mean temperature could then be plotted for the day of the year in which the station data was obtained. As an example, Figure 2 shows a scatter plot of the mean temperatures over the upper 30 m for the 241 days of the year in which at least one temperature station was recorded in region 1.The annual temperature curves to be explained next for both the earlier 1912–1983 period of study and this 1985–2013 study are also shown in Figure 2.

The annual temperature curves are constructed by using a regression scheme to fit a continuous annual temperature function to the integrated temperature data using the method of least squares. The final temperature functions are all of the form:

$$T(x) = M+A1 \sin(0.0172x+B1) + A2 \sin(0.0344x+B2) + A3 \sin(0.0516x+B3) \quad (1)$$

where x is the day number of the year and M,A1,A2,A3,B1,B2,B3 are the parameters which were computed from the regression scheme. The three sine functions are calculated in radians and the temperature T(x) gives the temperature in degrees centigrade. This temperature function was simplified from the first seven terms of the truncated Fourier series:

$$T(x) = M + \sum_{n=1}^{n=3}\left[a_n \sin\left(\frac{n\pi x}{p}\right) + b_n \cos\left(\frac{n\pi x}{p}\right)\right] \quad (2)$$

with period 2p=365 days. Equation (1) is derived from (2) by using the trigonometric identity

$$C_1 \sin(\theta) + C_2 \cos(\theta) = \sqrt{C_1^2 + C_2^2}\ \sin(\theta + k) \quad (3)$$

where $\arctan(k)=C_2/C_1$.

The coefficients and lag angles are computed by the least squares method rather than through the use of the Fourier integral, partly due to the fact that the temperature data is not evenly spaced in time and can lead to poor approximations in the integration for determining some of the coefficients. The use of least squares in place of computing Fourier coefficients is further explained by a well known result that Fourier coefficients give the best least-squares fit for the orthogonal expansion of the type of function described here. Hence, Fourier coefficients and least squares are closely bound.

The decision to express T(x) in terms of the first three harmonics on a Fourier series is based on several factors. For the purpose of comparisons among regions and ease of applications, such as in computer modeling, it is desirable to have a single function type which produces accurate results for each season in each of the 12 regions. The temperature should accurately describe early spring data, when vernal surface warming initiates vertical mixing and surface turnover, as well as the autumn data when surface and intermediate layers begin to cool. The length of the warming and cooling cycles, which vary among regions, should be reflected in the temperature function as well. To achieve these objectives, the temperature data for a given region was first regressed using only the sine term of the first harmonic,

$$T(x) = M+C1 \sin(0.0172x) \quad (4)$$

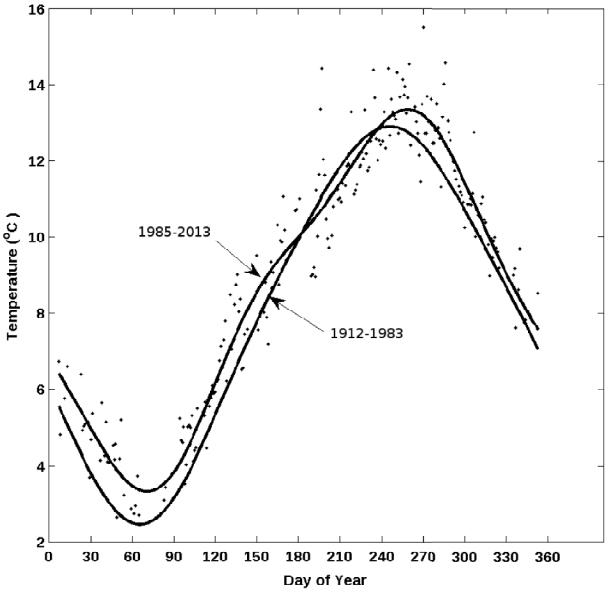

Fig 2. Integrated temperature data over the upper 30 m for each of the 241 acceptable days of the year. The corresponding fitted annual temperature curve over the upper 30 m in Region 1 is shown for 1985–2013. For comparison, the fitted curve from the 1912–1983 data is also shown.

The coefficient C1 was then examined using the null hypothesis that C1=0 against the hypothesis that C1≠0. At the 95% confidence interval, C1 was found to be significant and the cosine term was then added and the same data was regressed onto the function

$$T(x) = M+C1 \sin(0.0172x) +C2 \cos(0.0172x) \quad (5)$$

Again, C2 was found to be significant and included in the temperature function. The identity in equation (3) is applied to express equation (5) in the form

$$T(x) = M+A1 \sin(0.0172x+B1) \quad (6)$$

This first harmonic with a period of 365 days is the dominate harmonic in equation (1). It may be regarded as a first approximation to the annual fluctuation in temperature about the mean, M. But equation 6 would show the length of the warming and cooling cycles to be the same 6 months in each of the 12 regions. Moreover, equation (6) provides a less accurate fit in the spring and autumn data. The addition of the terms in the second harmonic to equation (6) were also found to be significant at the 95% confidence level, and provided a better fit overall. However, the sum of squares due to the error for just these two harmonics was most prevalent in spring and autumn. The addition of the third harmonic reduced the error and provided a

better overall fit, especially in the coastal regions where the amplitude of the third harmonic, A3, can exceed that of the second harmonic, A2. Although the third harmonic contributes less than 0.5˚C in the computation of any of the temperature functions, it is statistically significant in some regions, and modestly improves the fit in others. When additional harmonic terms were added to the first three harmonics, an analysis of their coefficients lead to their rejection at the 95% confidence interval. Also, it should be mentioned that there can be more than one combination of these functions when each function is added to the regression scheme in different orders. The functions chosen here were among the most statistically acceptable. As an illustration, Figure 2 shows the fitted temperature function over the upper 30 m corresponding to the averaged temperature data for region 1. The temperature function for the period 1985–2013 shown in Figure 2 is:

$$T(x) = 8.48 - 4.57 \sin(0.0172x+0.43) - 0.25 \sin(0.0344x+0.02) + 0.49 \sin(0.0516x+0.57) \quad (7)$$

Figure 2 also shows the temperature function that was fit to the 1912–1983 data set in True and Wiitala (1990) which is:

$$T(x) = 7.92 - 4.97 \sin(0.0172x+0.47) - 0.25 \sin(0.0344x-0.91) + 0.25 \sin(0.0516x+1.31) \quad (8)$$

The mean temperature in region 1 for 1985–2013 is about 0.56ºC warmer than in 1912–1983.

The information in Table 2 gives the values of the parameters M,A1,A2,A3,B1,B2 and B3 which are used in the temperature function T(x) for each of the 12 regions for the upper 30 m. The table also includes the number of days in the year at which at least one suitable temperature station was recorded, the standard deviation about the mean, M, the correlation coefficient and the days when the temperature function shows its annual minimum and maximum temperature in the given region. Table 3 gives the same results for temperature functions in the intermediate layer 30–70 m. The last row in Tables 2 and 3 give the temperature functions for region SS, the Scotian Shelf, which will be discussed later.

Table 2. Annual temperature functions integrated over the depth interval 0-30 m. The function is: $T(x) = M+A1 \sin(0.0172x+B1)+A2 \sin(0.0344x+B2)+A3 \sin(0.0516x+B3)$ where x=day number.

Region	No. of days	Standard deviation (SD)	Correlation coefficient (R)	M	A1	B1	A2	B2	A3	B3	Minimum temp (ºC)	Day number	Maximum temp (ºC)	Day number
1	241	0.79	0.97	8.48	-4.57	0.43	-0.25	0.02	0.49	0.57	3.32	70	13.35	259
2	151	0.86	0.96	7.76	-4.57	0.34	-0.17	-0.97	0.42	0.28	2.66	77	12.53	261
3	124	0.80	0.95	7.52	-3.77	0.19	-0.26	-0.77	0.36	0.82	3.14	76	11.39	262
4	312	0.65	0.98	7.24	-4.82	0.37	-0.17	0.38	0.14	1.49	2.21	65	12.13	254
5	266	1.22	0.93	6.79	-4.37	0.32	-0.23	0.44	0.29	-1.14	2.50	77	11.15	272
6	194	1.03	0.96	8.36	-4.63	0.43	0.34	0.11	0.05	0.53	3.88	75	13.28	245
7	291	0.95	0.97	8.76	-5.31	0.41	0.41	-0.28	0.10	0.93	3.70	73	14.54	248
8	338	0.61	0.99	9.70	-5.43	0.36	0.46	-1.48	0.16	-0.78	4.68	69	15.52	261
9	202	0.90	0.97	9.66	-5.32	0.45	0.51	-0.26	0.28	0.25	4.56	77	15.58	250
10	266	0.80	0.98	9.61	-5.30	0.50	0.74	-0.23	0.30	0.54	4.67	76	15.78	246
11	243	0.95	0.97	8.87	-4.79	0.43	0.42	0.16	0.31	0.33	4.01	79	14.11	250
12	287	1.04	0.96	8.51	-4.76	0.50	-0.56	0.61	0.49	0.16	3.41	66	13.63	264
SS	334	0.91	0.98	7.01	-6.80	0.37	-0.57	1.45	0.23	-0.23	0.52	68	14.37	262

Results and Discussion

The primary purpose of this work has been to offer a process for comparing future warming and cooling trends in various regions of the Gulf of Maine against standard or benchmark annual temperature curves based on historical data. These temperature functions for different regions may be plotted and compared to illustrate seasonal and geographical variability. In particular, they can be used for comparison with future temperature data surveys to determine cooling and warming anomalies in various topographic areas of the Gulf. Hopkins and Garfield (1979) selected the upper 50 m as the Maine Surface Water, with a temperature-salinity envelope which includes that of the Maine Intermediate Water having a depth range 50–120 m. For this study, the surface layer has been further divided into the 0–30 m and 30–70 m depth ranges. This division was partly influenced by biologists who were interested in temperature variability in a shallow upper layer. For con-

Table 3. Annual temperature functions integrated over the depth interval 30–70 m. The function is:
T(x) = M+A1 sin(0.0172x+B1)+A2 sin(0.0344x+B2)+A3 sin(0.0516x+B3) where x = day number.

Region	No. of days	Standard deviation (SD)	Correlation coefficient (R)	M	A1	B1	A2	B2	A3	B3	Minimum temp (°C)	Day number	Maximum temp (°C)	Day number
1	215	0.85	0.92	6.70	-2.72	-0.23	-0.68	-0.10	0.07	1.12	3.83	77	9.79	303
2	133	0.94	0.94	7.21	-3.70	0.11	-0.21	0.76	0.34	-0.52	3.37	89	11.34	277
3	122	0.76	0.95	7.26	-3.34	0.06	-0.28	-0.13	0.16	1.27	3.67	76	10.60	272
4	296	0.67	0.97	6.77	-4.13	0.15	-0.40	0.10	0.05	0.31	2.46	74	10.95	276
5	252	1.02	0.93	6.28	-3.43	0.19	-0.49	0.52	0.18	-0.94	2.88	72	10.03	280
6	190	0.81	0.93	7.03	-2.77	-0.05	-0.44	0.17	-0.04	1.08	4.28	77	10.03	292
7	292	0.83	0.92	7.19	-2.67	-0.08	-0.41	0.19	-0.12	1.45	4.61	84	10.17	294
8	335	0.72	0.98	9.26	-4.84	0.29	-0.59	1.01	0.31	-0.82	4.70	72	14.60	273
9	197	1.02	0.88	7.21	-2.33	-0.23	-0.62	0.18	0.09	-0.40	4.90	79	10.08	298
10	261	0.66	0.92	6.69	-2.09	-0.47	-0.67	-0.02	-0.08	0.51	4.90	81	9.45	313
11	239	0.74	0.94	6.90	-2.59	-0.21	-0.58	0.05	0.10	-1.31	4.35	84	9.99	300
12	258	0.85	0.92	6.21	-2.45	-0.26	-0.94	0.23	-0.21	1.20	3.97	65	9.68	305
SS	329	0.92	0.91	3.78	-2.49	-0.33	-1.01	-0.19	-0.25	-0.23	1.12	66	7.15	319

venience, the annual temperature functions summarized in Tables 2 and 3 will be referred to as the standard when compared with temperatures from different time periods.

The results of this work as summarized in Tables 2 and 3 include high correlation coefficients for fitting the temperature functions to the WOD13 data. The results for goodness-of-fit where encouraging and residuals were generally distributed evenly about the mean. The standard deviation among the twelve regions varied from 0.61ºC to 1.22ºC in the upper 30 m, and 0.66ºC to 1.02ºC in the 30–70 m layer. The column labeled M gives the annual mean temperature for each region. In the 0–30 m layer, region 5 south of Yarmouth, Nova Scotia showed the coldest mean temperature, 6.79ºC followed by region 4 for the Bay of Fundy at 7.24ºC. Coastal regions 2 and 3 were only slightly warmer. The warmest regions in the upper layer were the offshore regions 8, Georges Bank at 9.70ºC and region 9 over Roger's Basin at 9.66ºC. In the 30–70 m layer, region 5 was again the coldest at 6.28ºC, while the warmest was on Georges Bank, region 8 again at 9.26ºC.

The columns in Tables 2 and 3 for the minimum and maximum temperatures show the amplitude of variability among the regions. Generally, the lowest temperatures occur in March and the highest temperatures occur in September. In the 0–30 m layer, the annual temperature increased 8.25ºC in coastal region 3, and 11.11ºC over Wilkinson Basin, region 10. In the 30–70 m layer, annual temperature increased 4.55ºC in region 10 over Wilkinson Basin, and 9.9ºC over Georges Bank, region 8. During the warming period, temperatures in all regions generally increase at about

0.055ºC/day in the 0–30 m layer, and about 0.031ºC/day in the 30–70 m layer.

The Day numbers in Tables 2 and 3 can also be used to examine the length of the warming and cooling cycles for each of the regions. The warming cycles in the 0–30 m layer varied from 170 days in regions 6 and 10 over Jordan and Wilkinson Basins, to 198 days in Cape Cod Bay, region 12. For the 30–70 m layer, the warming cycle varied from 188 days in coastal region 2 to 240 days again in Cape Cod Bay. Generally, except for Georges Bank, the warming cycle in the surface layer was shorter offshore and over basins, where tidal mixing is reduced.

The temperature functions described here show an increase in the annual mean temperatures for most of the regions that were developed for the 1912–1983 period by True and Wiitala (1990). The differences in mean temperature for the surface layer 0–30 m and intermediate layer 30–70 m are shown in Table 4. The greatest increases occurred along the Maine coast, regions 1 and 2, and on Georges Bank, region 8 for both depth layers. On the other hand, region 5, where SSW enters the GOM between Cape Sable in Nova Scotia and Browns Bank, shows an overall decrease in mean temperatures in both the surface and intermediate layers. This temperature decrease corresponds with that of Smith *et al.* (2012) where, during the early 2000s, there was roughly a 40% increase of Scotian Shelf Water entering region 5 around Cape Sable into the GOM

Table 4. The difference in mean temperatures from 1912–1983 to 1985–2013 temperature functions for each region at the two layers 0–30 m and 30–70 m. Positive entries indicate an increase in mean temperature from 1912–1983 to 1985–2013.

	Region											
Depths	1	2	3	4	5	6	7	8	9	10	11	12
0–30 m	0.56	0.69	0.43	0.44	-0.24	0.21	0.01	0.48	-0.01	0.15	0.34	0.27
30–70 m	0.37	0.45	0.22	-0.06	-0.54	0.11	-0.02	0.41	0.08	0.12	0.18	0.07

compared with the 90s. Such an increase of colder SSW into region 5 would be reflected in the annual temperature function that was created for that region.

As an illustration, the mean annual temperature functions might be used to compare temperatures from a hydrographic survey or satellite data over a short time period relative to the 1985–2013 time period. For example, during 2003–2005, temperatures on the Scotian Shelf were cold relative to the period 1971–2000. The Department of Fisheries and Oceans Canada (DFO, 2004) reported that sea ice cover east of Cabot Strait during the first part of 2003 was twice the normal cover relative to the 1971–2000 period. The first part of 2003 marks the beginning of a decrease in temperatures on the Scotian Shelf, where the water was slightly colder and saltier than normal. The St. Andrews, N.B. annual surface temperature was 0.6ºC below normal and 1.8ºC colder than normal at Halifax, N.S. For 2004, Petrie *et al*. (2005) report a continuation of below-normal temperatures at St. Andrews and Halifax. Also, the cold intermediate layer on the Scotian Shelf was colder and thicker than normal from 50 m to the bottom. The northern edge of the Gulf Stream current moved about 20 km south of its mean position, leaving room for a stronger southern flow of the Labrador current.

Tracking water types through the GOM certainly requires more parameters than temperature alone. But we can start with the eastern GOM and search through adjacent regions to compare water temperatures during 2003–2005 with the 1985–2013 annual temperature functions. In Jordan basin, region 6, there is a moored buoy, buoy M01, whose data is collected and managed by the University of Maine Ocean Observing System (UMOOS, www.umoos.org). This buoy provides hourly temperature and salinity data at the depths 1, 20, 50, 100, 150, 200 and 250 m, beginning in July, 2003. Also, UMOOS buoy N01 on the east edge of the Northeast Channel, and the eastern part of region 7, has been recording temperature and salinity at similar depths beginning in June 2004. The data from these two buoys were cleaned and integrated to obtain a daily mean temperature for each day of each month of each year. The plots in Figure 3 compare the 30–70 m annual temperature functions for Jordan's and George's Basin (regions 6 and 7) with the 50 m temperature recordings from the two buoys during the period 2003–2005 for Jordan's and 2004–2005 for Georges Basin. For Jordan Basin, the buoy data for 2003–2005 shows a mean annual temperature of 1.17ºC below the mean of the annual temperature function for 1985–2013. Similarly, the buoy data in Georges Basin is 1.21ºC below the 1985–2013 annual temperature mean. In both cases, the buoy data at 50 m show the temperatures to be considerably colder during the summer warming season. In addition to comparing the buoy data available in regions 6 and 7 with the annual temperature curves, the WOD13 data for 2003–2005 from these regions were also compared (not shown). The results are the same, with every 30–70 m integrated temperature plot lying below the annual temperature curves. The coastal regions 2 and 3 for 2004–2005 also showed annual mean temperatures slightly more than 1ºC below the standard at both the 0–30 m and 30–70 m depths. Also, the annual mean temperatures for 2004–2005 in region 11 were below the standard by slightly more than 1ºC. This may be caused by transport out of adjacent region 2 by the western Maine coastal current. Region 9, Roger's Basin, just west of George's Basin, was not affected by the colder temperatures in adjacent regions. The remaining regions did not show significant temperature decreases for 2003–2005.

As another illustration, Townsend *et al.*(2015) have examined the data from buoy M01 at the lower depths of 100, 150, 200 and 250 m. Their study uses temperature, salinity, nitrates and silicates to try to determine the sources of water that enter Jordan Basin. They find that the proportions of the three water masses into the GOM lead to considerable T/S variability in Jordan Basin at these lower depths. By analyzing the data from the UMOOS buoy N01 on the east edge of the Northeast Channel, they argue that much of the deeper water in Jordan Basin is of Northeast Channel origin. In particular, during the period 2003 to 2014, they observed numerous fluctuations in temperature and salinity over time periods of 6 months to years. But from mid 2009 to 2014 the data showed a period of increasing temperature and salinity, with a slight decrease in 2011. Water masses can enter Jordan Basin as surface water from SSW along the south edge of Nova Scotia, and at various depths from the Northeast Channel and Georges Basin, region 7. Here, we look at the temperatures in the surface and intermediate layers for 2009–2013 and compare them with the standard for Jordan Basin by using the WOD13 data, which is sufficient to construct temperature functions like those in equation (1). Unlike the data from the M01

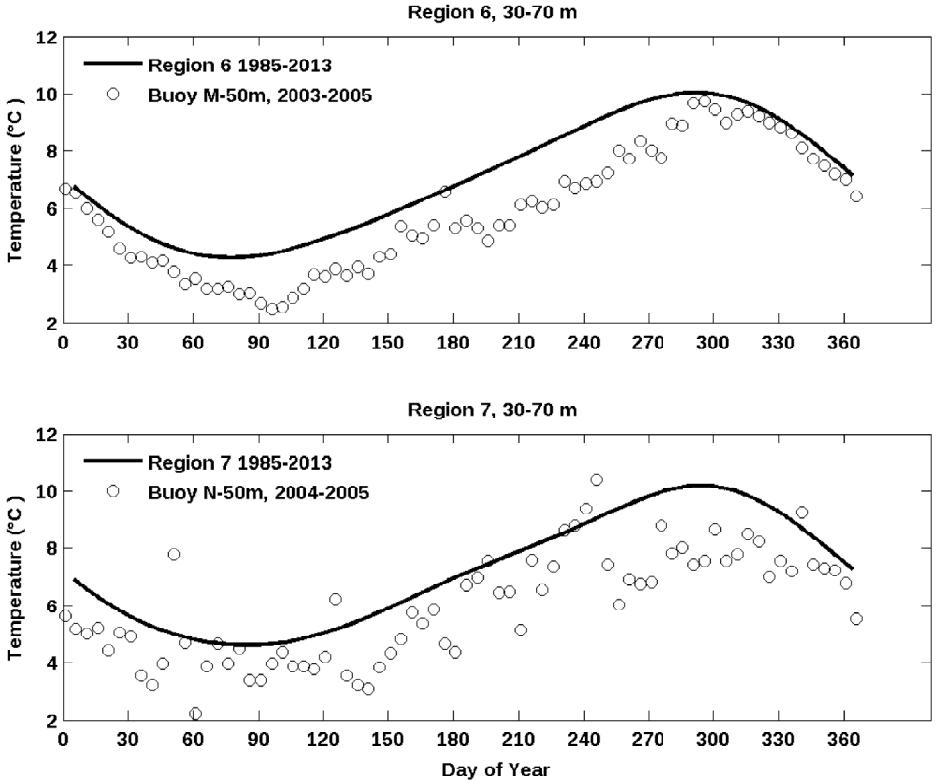

Fig 3. Upper figure: the annual temperature curve in region 6 (Jordan's Basin) in the intermediate layer 30–70 m is compared with the 50 m temperature data from Buoy N for 2003–2005. Lower figure: similar to upper figure for region 7 (Georges Basin) with temperature data from Buoy M for 2004–2005.

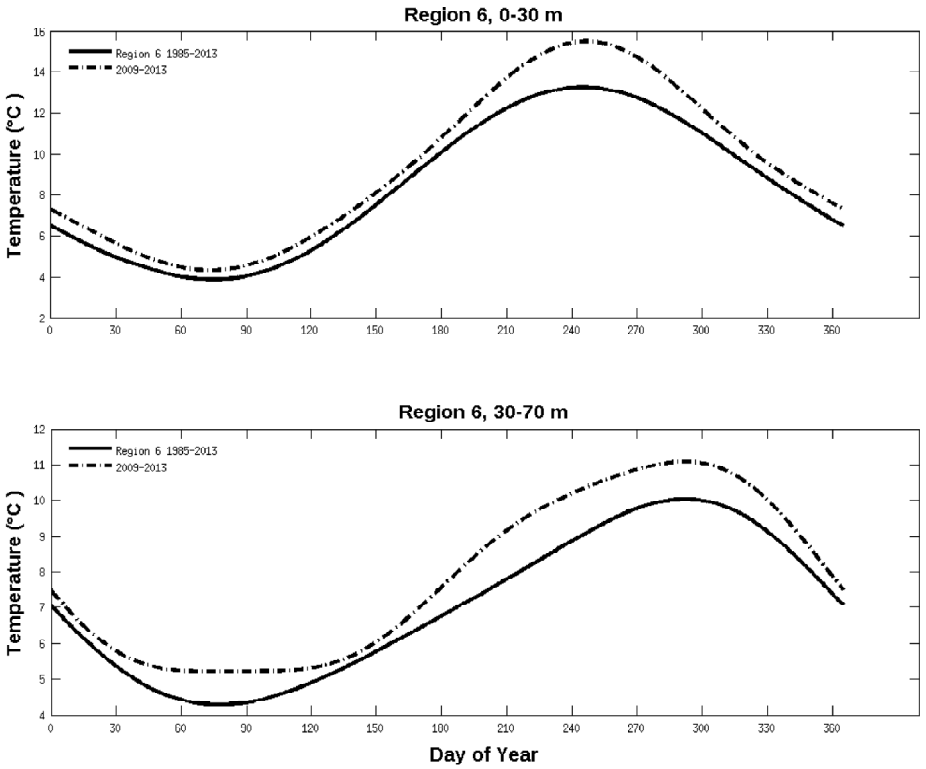

Fig 4. Upper figure: the annual temperature curve in region 6 (Jordan's Basin) in the surface layer 0–30 m for 1985–2013 is compared with the annual temperature curve for the warmer period 2009–2013. Lower figure: similar to upper figure at the intermediate layer 30–70 m.

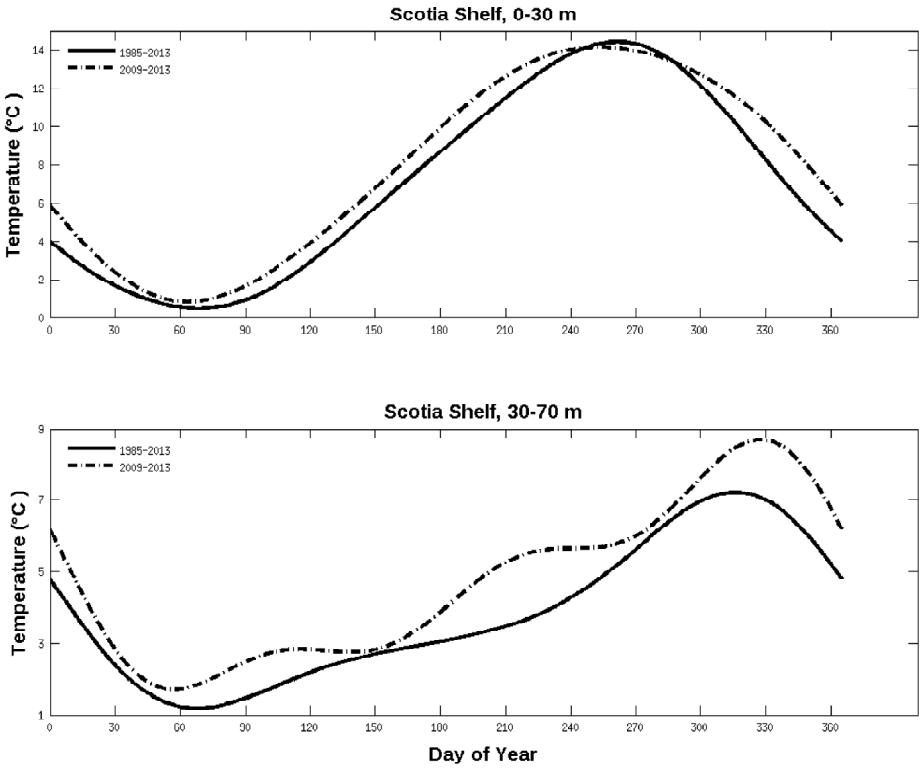

Fig 5. Upper figure: the annual temperature curve on the Scotian Shelf in the surface layer 0–30 m for 1985–2013 is compared with the annual temperature curve for the warmer period 2009–2013. Lower figure: similar to upper figure at the intermediate layer 30–70 m.

buoy, the WOD13 data set includes temperature data from stations all around Jordan Basin. The graphs in Figure 4 for Jordan Basin, region 6, show that temperatures in the upper layers were also generally higher throughout the period 2009–2013, with an annual mean increase of 1ºC in the depth interval 0–30 m, and 0.8ºC at 30–70 m relative to the 1985–2013 standard. Also, the same temperature curves were constructed for Region 5 east of Jordan Basin (not shown). Again, the temperatures for the period 2009–2013 were higher throughout the year than the standard, showing an annual mean increase of 1.5 ºC in the 0–30 m depth layer, and 1.4ºC in the 30–70 m layer. These results agree with Hebert (2014), who reported that temperatures at Lurcher Shoals in region 5 in 2012 (2013) were about 3.4ºC (1ºC) warmer at 50m than the 1981–2010 reference period. Hebert also reports that temperatures throughout the Scotian Shelf in 2013 were higher than the 1981–2010 means, and that 2012 was generally the warmest in 43 years.

In addition to the 12 regions used here for the GOM, the WOD13 data for the Scotian Shelf inside the1000 m isobath for 1985–2013 was also processed the same way as the 12 GOM regions. The annual temperature functions appear at the end of Tables 2 and 3, labeled SS. These functions were derived from the rectangular region of latitude 43.0 to 44.5N, and longitude 63.5 to 65.5W off Halifax, Nova Scotia. During 1985–2013, 7,617 stations were recorded in the data set. For comparison, Figure 5 compares the mean annual temperature functions for the Scotian Shelf from tables 2 and 3 with temperature functions that were constructed from the WOD13 data on the shelf during the period 2009–2013. The temperatures for 2009–2013 at the 0–30 m layer are 0.89ºC higher than the 1985–2013 standard and 0.92ºC higher at the 30–70 m layer. These comparisons enforce the suggestions that cooling and warming trends on the southwestern Scotian Shelf lead to similar results at the surface and intermediate layers in the eastern GOM. Temperatures in the coastal regions 2 and 3 and Georges Bank, region 8 during 2009–2013 were also greater than the 1985–2013 standard by more than 1ºC, while changes in the other regions were insignificant.

It must be emphasized that the sources of water masses in basins and on coastal areas of the GOM certainly can't be determined from surface temperatures alone. For example, the water masses passing through Jordan Basin at different levels remains a difficult problem, even when temperature, salinity, nitrates, silicates and other parameters are known. The results of a numerical model may be necessary to do a thorough analysis of the pathways and volume transports

of SSW, WSW and LSW moving in and out of the various regions of the GOM. But the comparisons shown here, along with similar testing in other time periods, illustrate that the annual temperature functions in Tables 2 and 3 are reasonably effective indicators of typical or standard annual temperature curves for the 12 regions represented in the Gulf of Maine.

References

BOYER, T. P., J. I. ANTONOV, O. K. BARANOVA, C. COLEMAN, H. E. GARCIA, A. GRODSKY, D. R. JOHNSON, R. A. LOCARNINI, A. V. MISHONOV, T. D. O'BRIEN, C. R. PAVER, J. R. REAGAN, D. SEIDOV, I. V. SMOLYAR, and M. M. ZWENG, 2013. World Ocean Database 2013, NOAA Atlas NESDIS 72, S. Levitus, Ed., A. Mishonov, Technical Ed.; Silver Spring, MD, 209 p., https://doi.org/10.7289/V5NZ85MT. Available at http://www.nodc.noaa.gov/about/oceanclimate.html

COLBOURNE, E. B. 2004. Decadel Changes in the Ocean Climate in Newfoundland and Labrador Waters from the 1950s to the 1990s. *Journal of Northwest Atlantic Fisheries* Science, **Vol. 34**: 41–59. https://doi.org/10.2960/J.v34.m478

DFO, 2004. State of the Ocean 2003: Physical Oceanographic Conditions on the Scotian Shelf, Bay of Fundy and Gulf of Maine. DFO Can. Sci. Advis. Sec. *Ecosystem Status Rep.* 2004/004.

DRINKWATER, K. F., and D. GILBERT. 2004. Hydrographic Variability in the Waters of the Gulf of St. Lawrence, the Scotian Shelf and the Eastern Gulf of Maine. (NAFO Subarea 4) During 1991–2000. *J. Northw. Atlan. Fish. Sci.*, **34**: 83–99. doi.org/10.2960/J.v34.m545.

DURBIN, E. G., R. G. CAMPBELL, and M. C. CASAS, *et al.* 2003. Interannual variation in phytoplankton blooms and zooplankton productivity and abundance in the Gulf of Maine during winter. *Mar. Ecol. Prog. Ser.*, **254**, 81–100.

GOURETSKI, V., and K. P. KOLTERMANN. 2007. How much is the ocean really warming?, *Geophys. Res. Lett.*, **34**, L01610, doi.org/10.1029/2006GL027834.

HEBERT, D., R. PETTIPAS, D. BRICKMAN, and M. DEVER. 2014. Meteorological, Sea Ice and Physical Oceanographic Conditions on the Scotian Shelf and in the Gulf of Maine during 2013. DFO Can. Sci. Advis. Sec. *Res. Doc* . 2014/070. v + 40 p.

HOPKINS, T. S. and N. GARFIELD. 1979. Gulf of Maine Intermediate Water. *J. Mar. Res.*, **37(1)**: 103–139.

JI, R., C. DAVIS, C. CHEN, D. TOWNSEND, D. MOUNTAIN, and R. BEARDSLEY. 2008. Modeling the influence of low-salinity water inflow on winter-spring phytoplankton dynamics in the Nova Scotian Shelf-Gulf of Maine region. *Journal of Plankton Research*, **Vol 30:** Num 12, 1399–1416 p.

JOHNSON, D. R., T. P. BOYER, H. E. GARCIA, R. A. LOCARNINI, O. K. BARANOVA, and M. M. ZWENG. 2013. World Ocean Database 2013 User's Manual. Sydney Levitus, *Ed.*; Alexey Mishonov,

TECHNICAL ED.; NODC Internal Report 22, NOAA Printing Office, Silver Spring, MD, 172 p. Available at http://www.nodc.noaa.gov/OC5/WOD13/docwod13.html.

LAUZIER, L. M. 1965. Long term temperature variations in the Scotian shelf area. *ICNAF Spec. Publ.*, **Vol 6**: 807–815.

LI, Y., R. HE, J. D. MCGILLICUDDY. 2014a. Seasonal and Interannual Variability in Gulf of Maine Hydrodynamics: 2002–2011. *Deep Sea Res Part 2 Top Stud Oceanogr*. 2014 **May**: 103–222. doi.org/10.1016/j.dsr2.2013.03.001

LI,Y., R. JI, P. S. FRATANTONI, C. CHEN, J. A. HARE, C. S. DAVIS, and R. C. BEARDSLEY. 2014b. Wind-induced interannual variability of sea level slope, along-shelf flow, and surface salinity on the Northwest Atlantic shelf. *J. Geophys. Res. Oceans*, **119**: 2462–2479.

PETRIE, B., R. G. PETTIPAS, W. M. PETRIE, and V. SOUKHOVTSEV. 2005. Physical oceanographic conditions on the Scotian Shelf and in the Gulf of Maine during 2004. *Cdn. Sci. Adv. Sec. Res. Doc.* 2005/21, 44 p.

SMITH, P. C., N. R. HOUGHTON, R. G. FAIRBANKS, and D. G. MOUNTAIN. 2001. Interannual variability of boundary fluxes and water mass properties in the Gulf of Maine and on Georges Bank: 1993–1997. *Deep-Sea Research*, **II 48**: 37–70. doi.org/10.1016/S0967-0645(00)00081-3

SMITH, P. C., N. R. PETTIGREW, P. YEATS, D. W. TOWNSEND and G. HAN. 2012. Regime Shift in the Gulf of Maine. In: Advancing an Ecosystem Approach in the Gulf of Maine. 415 p. Stephenson, R. L., J. H. Annala, J. A. Runge and M. Hall-Arber, (Eds). American Fisheries Society, Symposium 79, Bethesda, MD. p. 185–203

TOWNSEND, D. W., N. R. PETTIGREW, M. A. THOMAS, M. G. NEARY, D. J. MCGILLICUDDY, and J. O'DONNELL. 2015. Water Masses and Nutrient Fluxes to the Gulf of Maine. *J. Marine Research*, **Vol 73**, Numbers 3–4, May & July 2015, 93–122 p.(30)

TRUE, E. D., and S. A. WIITALA. 1990. Annual temperature curves in twelve regions of the Gulf of Maine. *NAFO Sci. Coun. Stud.*, **14**: 21–27.